Temporal relaxation of photoinduced nonequilibrium in niobium

Nathan Bluzer
Westinghouse Advanced Technology Laboratories, P.O. Box 1521, Baltimore, Maryland 21203
(Received 28 August 1991)

Transient photoimpedance responses (TPR) of nobium thin films are examined in the normal, transition, and superconducting states. The nobium sample's impedance is modulated by the photoabsorption of 300-fs, ~2-eV laser pulses with 0.002–1 μJ fluence. The samples, biased with a dc current, exhibit transient voltage signals corresponding to the photoinduced impedance transient. The TPR-signal amplitude and temporal dependence are analyzed in terms of the electron-photon, electron-phonon, electron-electron interactions and phonon trapping. Data interpretation is facilitated by comparing measurements of the TPR signal in all three states. Typically, the normal- and transition-state TPR signals are bolometric and are a manifestation of resistive impedance changes. At low laser fluences and in the zero-resistance superconducting state, the TPR signal is primarily due to kinetic inductance changes produced by the nonequilibrium quasiparticle generation and recombination processes strongly influenced by phonon trapping in the sample. At higher fluence, the niobium samples undergo temporary phase transitions that lead to more complicated TPR-signal responses, which we also analyze.

I. INTRODUCTION

Nonequilibrium properties of superconductors have received much experimental and theoretical attention. Such research is expected to provide a better understanding of the superconducting mechanism and also facilitate the application of these materials. Understanding nonequilibrium phenomena in superconductors requires study of the interactions in a coupled three-component system[1,2] of quasiparticles, Cooper pairs, and phonons. Conventionally, these interactions are studied by observing the relaxation of induced nonequilibrium distributions toward the thermal equilibrium distribution of quasiparticles, Cooper pairs, and phonon. The relaxation process is very complicated[2] and involves different time constants which includes (1) inelastic scattering of quasiparticles by electron-electron ($\tau_{e\text{-}e}$) and electron-phonon ($\tau_{e\text{-ph}}$) interactions, (2) quasiparticle recombination (τ_R) into pairs, (3) quasiparticle generation by phonon-induced pair breaking (τ_B), (4) phonon decay[3] by diffusion into the environment (τ_γ), and branch mixing (τ_Q). Macroscopically, these relaxation processes manifest themselves as the temporal dependence of the Cooper-pair density $n(t)$, the order-parameter time constant (τ_Δ), the value of the order parameter $\Delta(t)$, and the quasiparticle chemical potential $\mu_p(t)$. Much has been written on the subject[4,5] and the focus has been primarily on conditions near thermal equilibrium under low-energy excitations.[2] Larger deviations from the equilibrium state are represented by using an effective chemical potentials[6–8] (μ^* model) or an effective temperature[9] (T^* model). Thus far, inconclusive agreement exists between experimental results and the theoretical T^* or μ^* models.

Two tunnel junctions connected in tandem is the principal device structure used to study nonequilibrium in superconductors. One tunnel junction is used to produce the nonequilibrium conditions by electrically injecting quasiparticles into the inner superconducting layer, and the second junction is used to measure the branch imbalance[10–14] lifetime τ_Q within this layer.

The aforementioned methods[10–12] only induce a quasiparticle branch imbalance are not representative of optically induced nonequilibrium. Testardi[15] recognized that photoabsorption in a superconductor generates excess quasiparticles without a branch imbalance. With a sufficient optical generation of quasiparticles below T_C, a transition occurs from the zero-resistance superconducting state (ZRSS) into a resistive superconducting state (RSS). The RSS occurs below T_c when photoabsorption temporarily reduces the sample's critical-current capacity below the dc bias current. The observed resistance of the optically induced RSS gradually increases with light intensity from zero to the normal-state resistance thereby forming[7] a nonequilibrium resistive superconducting state wherein the normal and superconducting regions coexist. Photodepairing also causes a reduction of the order parameter[7] Δ and changes in the quasiparticle's chemical potential μ_p.

Unlike the RSS measurements,[7,15] Gittleman *et al.*[16] measured the quasiparticle lifetime, τ_R, in a ZRSS near T_c, where small changes in the quasiparticle population cause significant changes in the sample's kinetic inductance. When a superconductor near T_C is exposed to an ac electric field, it exhibits a frequency-dependent impedance related to the condensate's density and to the quasiparticle's lifetime.[17,18]

In this paper we present results on the nonequilibrium relaxation in Nb made with a transient photoimpedance response method.[19] Unlike the techniques,[10–16] these measurements were made in the normal, transition, and superconducting states. The synergism of having data from these three states results in better data analysis and interpretation.

The measurements above, at, and below T_C were all

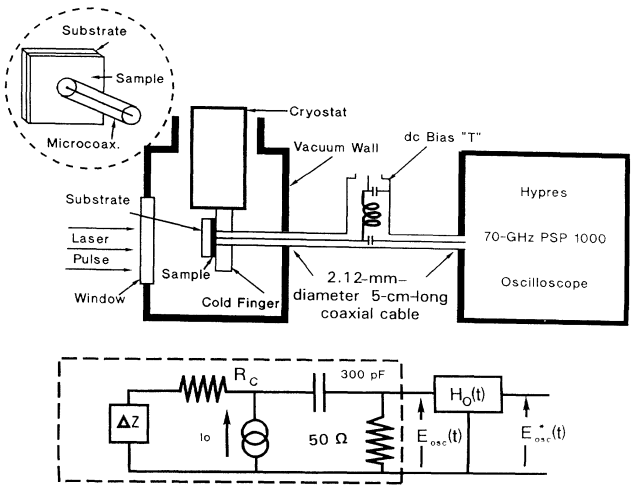

FIG. 1. TPR experimental setup includes sample inside a cryostat, microcoax, and bias T, and the Hypers oscilloscope. Inset illustrates the connection between the sample and the microcoax. The experiment's equivalent circuit has the sample (ΔZ) dc biased by I_0 through a contact resistance (R_C) and ac coupled to the oscilloscope [$H_0(t)$]. The oscilloscope input signal $E_{osc}(t)$ is modified by $H_0(t)$ to yield $E^*_{osc}(t)$.

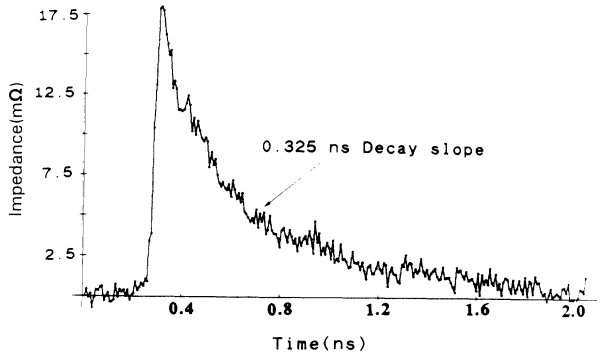

FIG. 2. Photoresponse at 140 K of a 20-nm Nb film on an Al_2O_3 substrate biased with 200 mA dc current and exposed to 1.31 μJ of laser fluence. The sharp rise corresponds to rapid heating of the Nb by electron-electron and electron-phonon processes. The slow decay portion corresponds to cooling with the phonon escaping into the substrate.

made the same way. At and above T_C the samples were resistive and below T_C the samples before photoabsorption were in the ZRSS. The wide bandwidth (70 GHz) and excellent sensitivity (50 μV) of the experimental setup (see Fig. 1) facilitated data taking. The Nb samples formed an electrical short across the end of a microcoax illustrated in Fig. 1. A dc bias current (1–150 mA) flowed through the samples during measurements. Exposing the samples to a 300 fs $\approx$2 eV laser pulse (2 to μJ) produces transient in the sample's impedance which appear as a transient voltage signal. In this paper, we describe and interpret the TPR signals observed between 6 and 200 K on a Hypers oscilloscope.

II. NORMAL-STATE PHOTORESPONSE

A. Experimental data

The normal-state TPR signal from Nb has been examined in terms of rise time, decay time, and amplitude. The normal-state TPR signal from Nb is similar to the results obtained from[20,21] $YBa_2Cu_3O_7$. We find that the normal-state TPR signal is consistent with a bolometric response and is not anomalous[22] if the specific heat of the niobium energies is taken into account. Typically, the TPR signal exhibits a sharp positive rise (< 40 ps) followed by more gradual (> 500 ps) decay back to the equilibrium resistance (see Fig. 2). The decay slope for several Nb films studied, listed in Table I, is plotted for three films in Fig. 3. Very little temperature dependence is observed between 40 and 200 K. The thinner Nb film, No. 3, does indicate a trend toward a faster decay slope than the thicker Nb films, Nos. 2 and 4. No dependence of the decay slope on the substrate material is observed. The photoresponse amplitude, normalized by the laser's fluence, is plotted in Fig. 4 and is representative of the films studied. Typically, the photoresponse amplitude increases as the temperature decreases.

Interpretation of these data requires examination of the temporal and amplitude characteristics of the TPR signals in terms of the thermalization processes inside the Nb samples. Previously,[19] it was demonstrated that the TPR signal, in the normal state, corresponds to the resistive photoinduced impedance transients revealed by the dc bias current flowing through the sample. Accordingly, the normal-state data analysis is based on resistive transients in the sample's impedance.

B. Temporal dependence of the normal-state TPR signal

The temporal dependence of the TPR signal is a manifestation of the thermalization process initiated with the

TABLE I. Characteristics of niobium samples used in this experiment.

Sample and number	T_C (K)	ΔT_C (mK)	ρ (300 K) $\mu\Omega$ cm	ρ (T_C) $\mu\Omega$ cm	d (nm)	$R_N(T_C)$ (Ω)	$\lambda_{KI}(0)$ (fH)	Substrate	Deposition method	$\frac{\Delta\rho}{\Delta T}$ $\mu\Omega$ cm/K $T > T_C$
Nb 1	9.2	< 50	16	0.5	40	0.023	10	$LaAlO_3$	dc sputtered	0.057
Nb 2	9.2	< 50	16	0.5	40	0.023	10	Al_2O_3	dc sputtered	0.057
Nb 3	8.9	< 50	16	0.9	20	0.083	20	Al_2O_3	dc sputtered	0.055
Nb 4	9.2	< 50	16	0.5	40	0.023	10	$LaAlO_3$	dc sputtered	0.057

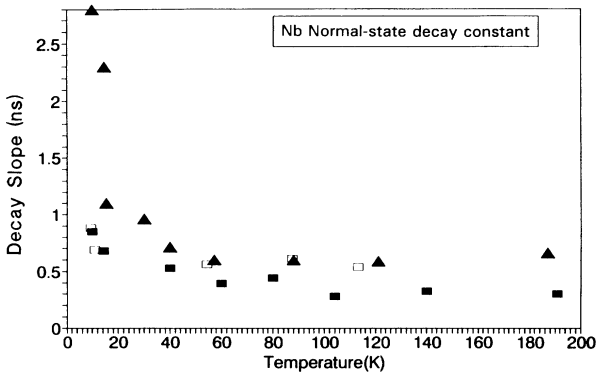

FIG. 3. The TPR-signal decay slope plotted for three Nb films: ■, No. 3; □, No. 2, and Δ, No. 4. The decay slope shows very little temperature dependence between 40 and 200 K.

photoabsorption of a subpicosecond laser pulse. The thermalization process has been grouped into four regimes: (1) electron-photon interaction, (2) electron-electron interactions, (3) electron-phonon interactions, and (4) phonon escape form the thin film into the substrate. The TPR-signal amplitude and fast risetime are a manifestation of the speed of the first three regimes and is described below.

Initially, each 300-fs laser pulse is absorbed[23] in Nb by photoexciting electrons about 2 eV above the Fermi surface (E_F). The fast photoabsorption step ($<10^{-15}$ s) is followed by thermalization[24] occurring first by electron-electron interaction (τ_{ee}) and next by electron-phonon interaction ($\tau_{e\text{-ph}}$). These time constants[24,25] τ_{ee} and $\tau_{e\text{-ph}}$ are, proportional to $(1/\varepsilon^2)$ and $(1/\Omega^3)$ respectively, where ε is the electron's excess energy above E_F and $\hbar\Omega$ is the maximum energy of the emitted phonons.[24]

$$\tau_{ee}=\left[\frac{\kappa}{P_F}+\frac{16}{\pi}\frac{q_D}{P_F}(\beta^2+\beta)\right]^{-1}\frac{64}{\pi^4}\frac{h}{e}\frac{E_F}{\varepsilon^2}\ , \tag{1a}$$

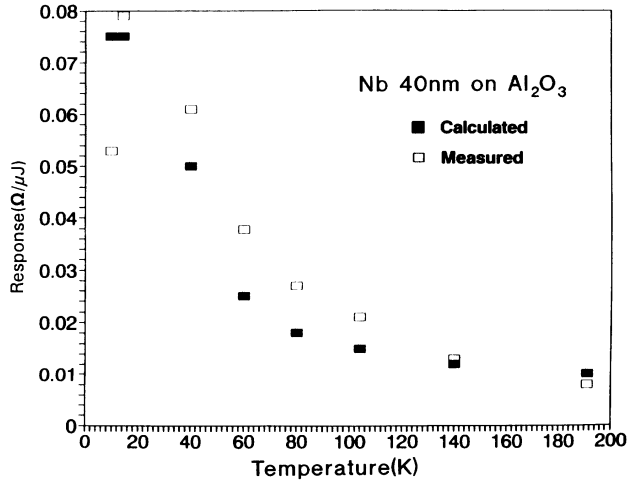

FIG. 4. Photoresponse of Nb thin-film sample No. 3 showing good agreement between measured and calculated photoresponse based on a bolometric model.

$$\tau_{e\text{-ph}}=\frac{1}{(7\pi)\xi(3)\beta}\frac{h}{e}\frac{(P_F u_a)^2}{(\hbar\Omega)^3}\ . \tag{1b}$$

These equations are valid for $\sim 10(k\Theta_D)>\varepsilon>kT$ and $\hbar\Omega>kT$ and the energy terms are all expressed in electron-volt units. The constants[26] (h/e), β, and $\xi(3)$ are, equal to 4.2×10^{-15} J s/Coulomb, 0.5, and 1.2, respectively. The other variables in Eqs. (1a) and (1b) are the following: P_F represents the momentum at the Fermi surface, q_D represents the Debye phonon momentum u_a, represents the longitudinal phonon velocity, and κ (Ref. 26) represents the Thomas-Fermi screening momentum. For normal metals[26] we estimate $\kappa\approx P_F$ and $p_F u_a\approx k\Theta_D$. Numerical values for (1a) and (1b) (Debye temperature[27] $\Theta_D=276$ K, $E_F=5.32$ eV, acoustic velocity[27] $u_a=5.32\times10^3$ m/s) are

$$\tau_{ee}\cong\frac{2.7\times10^{-15}}{\varepsilon^2}\ \text{s}\ , \tag{2a}$$

$$\tau_{e\text{-ph}}\cong\frac{1.8\times10^{-19}}{(\hbar\Omega)^3}\ \text{s}\ . \tag{2b}$$

These expressions [(2a) and (2b)] reveal very short (10^{-12} s) interaction times for electron-electron and electron-phonon processes. Thus, within a very short time, the photodeposited energy is converted into phonons. The TPR-signal short risetime is consistent with these calculations especially when the effects of the 70-GHz oscilloscope bandwidth and the 12-ps external trigger jitter are included.[19]

The decay slope of the TPR signal is typically much longer than the short rise time and is independent of the substrate material. This decay slope corresponds to a thermalization process and depends on the phonon escape time constant from the film into the substrate, τ_{es}. Little[28] and Anderson,[29] using only low-energy acoustic phonons, described an ideal model for this process. Using such a model, Kaplan[30] provided the relationship for the escape rate in terms of the phonon escape probability from the film into the substrate η, the phonon's velocity u_a,[27] and the film's thickness as

$$\tau_{es}=\frac{4d}{\eta u_a}\ . \tag{3}$$

The acoustic transmission probability from Nb into Al_2O_3 is calculated to be about $\eta\approx0.25$. For a 40-nm (20-nm) Nb film, the escape time τ_{cs} calculated is ≈120 ps (60 ps). These calculated values are a factor of 4 smaller then the measured values at higher ($T>40$ K) temperatures as evident in Fig. 3. This underestimate indicates the nonideal interface between the film and the substrate. Ideally, the interface should exhibit a thermal resistance[29,31,32] proportional to $1/T^3$ with the phonon escape time constant expected to follow a similar trend. It is evident from Fig. 3 that this is not the case for Nb and is similarly observed[20,33] for $YBa_2Cu_3O_7$. The temperature independence of the normal-state decay time constant indicates that, at higher temperature ($T>40$ K), the phonon wavelength is sufficiently short[34] (< nm) to be more sensitive to interface defects and hence no temperature

dependence is observed. However, it should be noted that, in this experiment, the phonons were generated from thermalization of hot electrons and thus, typically, their expected wavelength is shorter than expected of thermal equilibrium phonons. Consequently, the measured decay slope is expected to have no temperature dependence (as does the ideal acoustic model with a $1/T^3$ boundary-dependent resistance) and this is expected to persist for measurements even at lower temperatures. Overall, the decay time constant is consistent with thermal response as is corroborated from examining the TPR signal's positive amplitude.

C. Photoresponse amplitude in the normal state

The thermalization process of a 2-eV photoexcited electron is fast ($<$ 40 ps) compared to the phonon escape time from the film into the substrate. Thus, at the TPR-signal peak amplitude, all the energy from the hot electrons has been transferred to phonons. As will be shown, the TPR-signal amplitude is consistent with a change in the sample resistance produced by heating of the sample by ΔT degrees with the laser-pulse energy.

The normal-state photoresponse $\mathcal{R}(T)$ normalized by the laser's fluence $L(\mu J)$ can be expressed as

$$\mathcal{R}(T)\frac{1}{2\pi d}\ln\left[\frac{r_2}{r_1}\right]=\frac{0.184}{d}\frac{\Delta T}{L(\mu J)}\frac{\partial\rho(T)}{\partial T}\ , \tag{4}$$

where $r_2\approx 0.82$ mm and $r_1\approx 0.026$ mm are, respectively, the inner radius of the microcoax shield and the radius of the center conductor. The rise in the film temperature (ΔT) is expressed in terms of the film's relevant volume (V), the optical absorption[23] length (α), the laser beam cross section (A_L), the sample cross section (A_S), the sample specific heat[35] $C(T)$, and the optical reflection coefficient ($T_{\rm op}\cong 0.5$) as

$$\Delta T=\frac{L(\mu J)}{A_L}\frac{A_S}{C(T)V}[1-\exp(-\alpha d)]T_{\rm op}\ . \tag{5}$$

Combining Eqs. (4) and (5), the photoresponse amplitude is expressed as

$$\mathcal{R}(T)\cong\frac{0.107}{d}\frac{1-\exp(-\alpha d)}{C(T)}\frac{T_{\rm op}}{V}\frac{\partial\rho(T)}{\partial T}\ . \tag{6}$$

We have substituted for $A_L\approx 0.038$ cm^2 and $A_S\approx 0.022$ cm^2 to obtain Eq. (6). The value of the remaining terms in Eq. (6) have been obtained from experimental measurements on the film's resistivity. Typically the Nb samples have a room-temperature resistivity (16 $\mu\Omega$ cm) independent of film thickness. However, the resistivity ratio, $r_{\rm RR}=\rho(300\ {\rm K})/\rho(10\ {\rm K})$, is larger for the thicker samples. For 40- and 20-nm thick Nb films, the $r_{\rm RR}$ is 27 and 17, respectively, with the resistivity decreasing linearly with temperature between 300 and about 25 K (see values in Table I). Between 25 and 10 K the change in the Nb film resistance is much smaller (5$\times$) than between 25 and 300 K. At T_C, a sharp change ($\Delta T_c<50$ mK) occurred as the films became superconducting. Between 25 K and T_C, the Nb film resistance is dominated by surface and impurity scattering. Using these temperature-dependent resistivity values (see Table I) and the published values for the specific heat[35] and the optical absorption[23] (α) for Nb, comparisons are made between calculations and experimental measurements.

Figure 4 compares the measured and calculated photoresponse amplitudes. The calculated points in Fig. 4 were obtained assuming the bolometric model [Eqs. (4)–(6)] and good agreement is obtained between experiment and calculations. Similar plots and good agreement is obtained for the other Nb films listed in Table I. In all cases the agreement between the calculated and measured values were typically within a factor of 2 with the worst case being a factor of 4. Such reasonable agreement between the measurements and calculations is strong support for the bolometric photoresponse.

III. TRANSITION-STATE PHOTORESPONSE

Measurements of the TPR-signal amplitude and relaxation slope at T_C is difficult because the narrow ($\approx$50 mK) transition temperature width made it difficult to set the sample's operating temperature exactly at T_C. This is not simplified by the dc bias current flowing through the niobium sample which reduces the transition temperature and broadens it width.[36] Typically the measurements at T_c are made by cooling the sample slightly below T_C and letting the laser fluence heat the sample through the transition temperature. This transient heating effect is observed only on the oscilloscope and is not observable with the silicon diode thermometer nor with the Tektronics digital voltmeter (DM501A), monitoring the sample's steady-state resistance.

The transition photoresponse data are analyzed assuming the photoabsorbed laser pulse energy thermalizes into phonons during the TPR-signal risetime as described by Eqs. (2a) and (2b). Within this short time a sufficient number of phonons and quasiparticles are generated to

TABLE II. TPR-signal amplitude about T_C of Nb thin films heated through T_C by the absorbed laser fluence. The calculated ΔT (K) film heating assumed all the absorbed fluence heated the lattice.

Sample No.	Response Ω Calculated	Response Ω Measured	Laser fluence (μJ)	Initial temp. (K)	Calculated heating ΔT (K) by laser	Slope (ns)
1	0.027	0.032	0.7	7.2	24	5.2
3	0.086	0.075	0.0044	8.08	1.1	2.11
4	0.027	0.025	0.024	8.46	3.3	2.26

cause the niobium samples to go thought their transition temperature. Thus, the TPR signal following the fast risetime is treated as being from a sample heated from the ZRSS past the RSS and the transition phase into the normal state. The calculated photoresponse amplitudes, with Eqs. (4)–(6) are given in Table II and are in very good agreement with the measured results. Typically at T_C the TRP signals are higher than the photoresponse amplitude in the normal state plotted in Fig. 4. This is expected since the largest change in resistance with temperature occurs at T_C.

IV. SUPERCONDUCTING STATE RESPONSE

In the superconducting state the TPR signal is more difficult to interpret because photoabsorption can cause the sample's impedance to transition temporarily out of the zero-resistance inductive state into the RSS, the transition state, and the normal state. The state into which the samples temporarily transition and the shape of the TPR-signal decay are very sensitive to laser fluence. Typically, samples undergoing a state change exhibit a TPR signal that cannot be described by a single decay time constant. It is inferred that, following the initial rise in the sample's temperature (see Table II and Fig. 5), the decay slope is a representation of the cooling process as the sample returns back to the ZRSS from an excited state. With sufficient laser fluence, this cooling process may take the sample from the normal state, through the transition state, through the RSS, back into the ZRSS.

The final stage of this thermalization process occurs as the sample cools from the ZRSS and the relaxation of this process is controlled by the order parameter[5,37–39] τ_Δ. Typically it is expected that the recombination of quasiparticles will be slowed down and dominated by the order-parameter time constant τ_Δ. At lower temperatures and for smaller laser fluences the sample will remain in the ZRSS following photoabsorption and this we describe first. All these cases are examined with the aid of the experimental transfer function.[19]

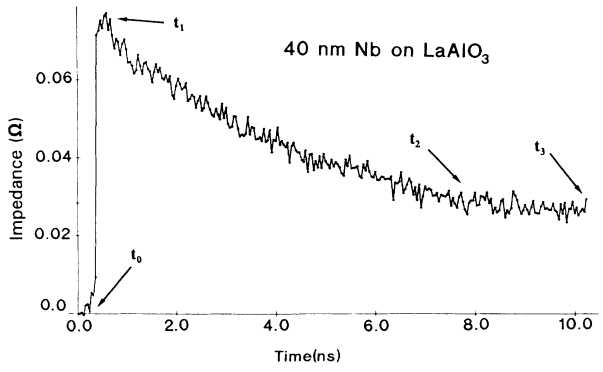

FIG. 5. TPR signal from a 40-nm Nb film on $LaAlO_3$ biased with 50.2 mA in the ZRSS at 7.2 K. Photoabsorption of 700 nJ at t_0 heats the sample into the normal state and about 30 K at t_1. As the Nb cools into the temperature-insensitive resistive region, at t_2 and between T_C and ≈ 25 K, the TPR signal exhibits a nonzero plateau [see Fig. 9(c)].

A. Thermalization in the zero-resistance state

In the zero-resistance state the output signal is generated from changes in the kinetic inductance, $L_{KI} \propto 1/n(t)$, revealed with the dc current (I_0) flowing through the sample[19] where $n(t)$ represents the time-dependent Cooper-pair density. The effect of the normal channel[40] is to act as an attenuator[19] on the signal produced by changes in the kinetic inductance. Neglecting the attenuation effects, the output voltage signal is approximated by

$$E_{\rm osc}(t) \approx I_0 \frac{dL_{\rm KI}}{dt} \approx I_0 \frac{d}{dt}\left[\frac{1}{n(t)}\right] . \tag{7}$$

The rate of change in the Cooper-pair density corresponds to the thermalization process and establishes the amplitude, polarity, and the temporal dependence of the TPR signal. With net quasiparticle[19–21] generation (recombination), the output signal is positive (negative). The peak TPR signal amplitude[19–21] $E_{\rm osc}(t)$ occurring at very short times ($t = 0_+ \approx 10^{-14}$ s) can be expressed in terms of the initial change in kinetic inductance ($\Delta\eta$) as

$$\Delta\eta \approx \frac{E_{\rm osc}(0_+)}{I_0}\frac{L_G}{Z_0} , \tag{8}$$

where $L_G \approx 30$ pH is the geometrical inductance[41] of the sample and $Z_0 = 50\Omega$ is the coax impedance. This inductance change depends on how many pairs, on average, have been broken immediately following photoabsorption and this is considered next.

Initially the 2-eV hot quasiparticles thermalize quickly by electron-electron interaction (cascading). During each cascading step each hot quasiparticle loses about half its excess energy. Specifically, for 2-eV photons the cascading process starts about E_F+2 eV and continue by discrete energy steps approximately as E_F+1 eV, $E_F+0.5$ eV, $E_F+0.25$ eV, $E_F+0.125$ eV, $E_F+0.067$ eV, $E_F+0.034$ eV, $E_F+0.016$ eV, and so on. At each succeeding cascading step the population of broken pairs doubles, the excess energy "ε" of each hot quasiparticle is halved, and the cascading process, proportional to $1/\varepsilon^2$, slows down. At a certain excess energy level it becomes more favorable for thermalization to continue through phonon emission instead of cascading. These emitted phonons will be (1) most energetic to speed up the thermalization process [$\tau_{e\text{-ph}} \propto (1/\hbar\Omega)^3$], (2) strongly coupled to the electrons, and (3) consistent with conservation of energy and momentum.

In niobium, the phonons most strongly coupled to the electrons are the 3.5×10^{12} Hz (15 meV) longitudinal phonons in the $\langle 111 \rangle$ direction[42,43] as evident from the need to use ten nearest neighbors to fit the experimental phonon dispersion[42,43] curves with the Born–von Kármán theory. This phonon linear momentum at 3.5×10^{12} Hz is 1.67×10^{24} kg m/s, or $\approx 2.6P_F$. To maintain momentum conservation,[27] only lower-energy phonons ($<$ 11 meV or 2.6×10^{12} Hz) can be emitted during thermalization. From the relative values of τ_{ee} and $\tau_{e\text{-ph}}$ (for $\hbar\Omega \cong 11$ meV), we estimate that the transition from cascading to phonon emission will occur be-

tween 0.030 and 0.016 meV. Thus, it is expected that each photoabsorbed photon will break between 64 and 128 Cooper pairs, or about 100 on average, by cascading before phonon emission begins. This is unlike $YBa_2Cu_3O_7$ where the presence of (≈ 50 meV) optical phonons[44,45,46] satisfy momentum requirements thereby allowing transition from cascading to phonon emission to occur earlier[21] (≈ 0.1 eV).

The thermalization process in niobium is illustrated in Fig. 6(a) where the temporal dependence of the Cooper-pair density is given for a sample starting in the ZRSS and exposed to a 300-fs laser pulse. Immediately following photoabsorption at t_0, the cascading process directly decreases the Cooper-pair density from n_0 to n_1 by time t_1. With cascading, the hot quasiparticles lose energy and it becomes more favorable for them to continue their thermalization by phonon emission at time t_1. After a short time ($<10^{-12}$ s), the cascading and phonon emission processes are completed to produce a nonequilibrium excess population of quasiparticles and phonons. The excess phonons, trapped in the Nb film by the thermal bottle neck, continue to increase the net quasiparticle population from time t_1 to time t_2. As enough phonons escape into the substrate, net quasiparticle recombination occurs from time t_2 to time t_3, where equilibrium is reestablished.

In Fig. 6(b), the solid-line trace illustrates the TPR-signal amplitude expected for the temporal changes in the Cooper-pair density shown in Fig. 6(a). The TPR-signal peak amplitude (at about t_1) occurs at the maximum quasiparticle generation rate. At low laser fluence levels, the peak TPR signal corresponds to a change in the kinetic inductance produced by the cascading process that breaks pairs directly and very quickly. With higher laser fluence levels, or near T_c, the niobium samples can be sufficiently heated to rapidly break additional pairs by phonon.

The ZRSS photoresponse amplitude $E_{\rm osc}(0_+)$, given by Eq. (8), is produced by sudden changes in the sample's kinetic inductance, $\Delta\eta$, occurring immediately following photoabsorption. Next, we compare the measured (e.g., Fig. 7) TPR-signal peak amplitude, $\mathcal{R}_M(T)$ given in Table III, to the calculated photoresponse amplitude $\mathcal{R}_C(T)$. These quantities, normalized by the laser's fluence $L(\mu J)$ and the initial inductance $L^0_{\rm KI}$, are given by

$$\mathcal{R}_M(T)=\frac{\Delta\eta}{L^0_{\rm KI}L(\mu J)}\ , \tag{9}$$

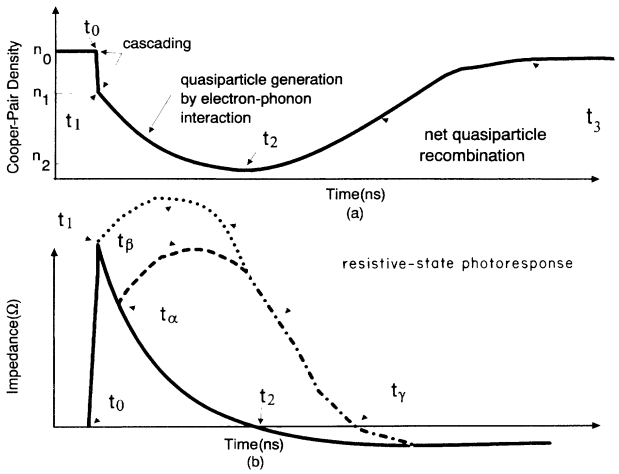

FIG. 6. (a) The Cooper-pair density with (b) the projected TPR signal vs time are given following photoabsorption at t_0.

$$\mathcal{R}_C(T)=\left[\frac{1}{n_1(T)}-\frac{1}{n_0(T)}\right]\frac{n_i}{L(\mu J)}\ , \tag{10}$$

where the Cooper-pair density at 0 K, $n_i\simeq 10^{22}$ cm^{-3}, is computed from the London penetration depth of Nb.[47] Also, $n_0(T)$ and $n_1(T)$ are, respectively, the Cooper-pair densities immediately before and after ($\simeq$ps) photoabsorption. Immediately after photoabsorption, two processes produce the initial reduction in the Cooper-pair density: cascading (n_C) and phonon pair breaking ($n_{\Delta T}$) (corresponding to the sudden increase in the sample's temperature by ΔT) giving $n_1(T)=n_0(T)-n_C-n_{\Delta T}$.

A rough estimate of

$$n_{\Delta T}=n_i[(T_{\rm op}+\Delta T)^4-(T_{\rm op})^4]/T_C^4$$

(see Table III) is made by using the two-fluid model[40] and assuming that the rise in the sample temperature, below T_C, can be made with Eq. (5). Since these measurements were made close to T_C, where the heat capacity of niobium is very small, the number of Cooper pairs broken by this process is significant and is given in Table III.

The number of broken pairs n_C produced by the cascading process are

$$n_C=100\frac{(10^{-6})[1-\exp(-\alpha d)]T_{\rm op}}{A_L d(3.2\times 10^{-19}\ \text{J/photon})}\ , \tag{11}$$

TABLE III. Comparisons between measured photoresponse $\mathcal{R}_M(T)$ and calculated photoresponse $\mathcal{R}_C(T)$. The transition temperature used is the zero current value given in Table I and the Cooper-pair density is 10^{22} pairs/cm^3. Because of the 238 kA/cm^2 bias current, the equilibrium T_C, of sample No. 1, is suppressed by 0.4 K.

Niobium sample number	Laser fluence (nJ)	Bias current (kA/cm^2)	$T_{\rm op}$ (K) of sample	ΔT (K) laser heating	$n_{\Delta T}$ (cm^{-3}) phonon generated	n_C (cm^{-3}) cascading generated	$\mathcal{R}_C$ (T) cascading & phonons	$\mathcal{R}_M$ (T)	Slope (ns)
1	7	238	6.25	1.27	2.79×10^{21}	6.3×10^{18}	113	163	0.83
3	3.7	62	6.0	1.26	2.36×10^{21}	8.0×10^{18}	142	242	0.85
4	3.7	31	6.0	0.85	1.26×10^{21}	3.3×10^{18}	63	294	0.65

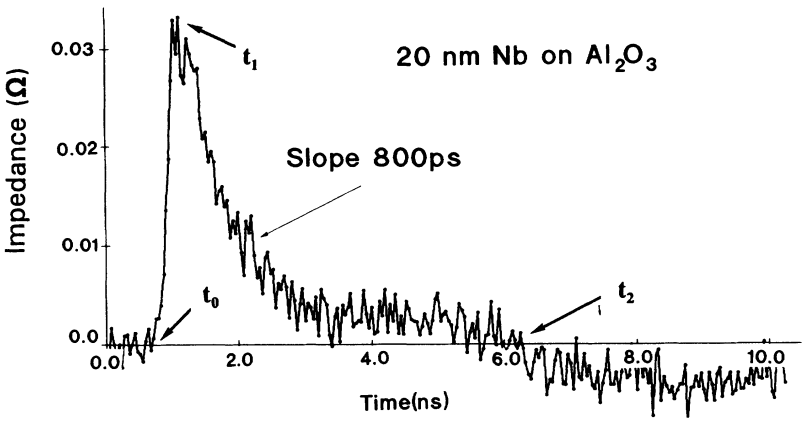

FIG. 7. TPR signal from sample No. 3 at 6 K biased with 19.6 ma and exposed to 3.7 nJ of laser fluence. In the ZRSS, photoabsorption produces the peak response (t_1) and a negative TPR signal (t_2) when a sufficient number of phonons escape into the substrate permitting net quasiparticle recombination.

where the leading coefficient, 100, corresponds to the estimated average number of Cooper pairs broken by cascading and the other terms have been previously introduced in Eq. (4). The computed $\mathcal{R}_c(T)$ and measured $\mathcal{R}_M(T)$ photoresponses are given in Table III and reasonable agreement is obtained considering how approximate our model is.

The ZRSS TPR-signal positive amplitude decay slope, listed in Table III, corresponds to the extrinsic pair-breaking time by phonons (τ_B^{ext}). Typically, $\tau_B^{\text{exp}} \approx 800$ ps is larger than the intrinsic pair-breaking time $\tau_B \approx 17$ ps as computed by Kaplan *et al.*[2] ($\tau_B^{\text{ext}} \approx 50\tau_B$). The longer τ_B^{ext} is due to the phonon trapping that produces a condition where quasiparticle generation and recombination are occurring in parallel with pair breaking dominating. After a sufficient number of phonons escape into the substrate, pair recombination will start to dominate, as is evident from the negative signal amplitude (e.g., Fig. 7). A large perturbation and the simultaneous generation and recombination of many quasiparticles makes the direct application of Kaplan *et al.*[2] insufficient and instead the Rothwarf-Taylor[3] equations are required.

The measured $\tau_B^{\text{ext}} \approx 800$ ps, longer than $\tau_B \approx 17$ ps, can be computed by asserting that, for every 100 Cooper pairs broken, by phonons, concurrently 98 Cooper pairs are reformed by quasiparticle recombination (i.e., $98\tau_R \approx 100\tau_B$) yielding $\tau_B^{\text{ext}} \approx 50\tau_B$. For $T/T_C > 0.75$, the intrinsic quasiparticle recombination is approximately $\tau_R \approx 25$ ps and τ_B varies from 7 ps ($T/T_C = 0.75$) all the way to infinity as T/T_C approaches unity. Given this range of τ_B, reasonable agreement is inferred between experiment and theory.

B. Thermalization in the resistive state

The simplest photoinduced phase transition is from the ZRSS to a RSS and back to a ZRSS.[20,21] Such transitions occur for $T < T_C$ and when the number of photodepaired Cooper pairs temporarily reduces the sample's critical-current capacity to a value below the sample's dc bias current. This transition can occur during the sharp TPR-signal risetime [dotted curve in Fig. 6(b)] or during the decaying portion of the ZRSS signal [dashed curve in Fig. 6(b)].

In a RSS, quasiparticle generating produces an increasing positive signal corresponding to increases in the sample resistance and the broad round peak is observed.[20,21] At the peak amplitude, represented by time t_β in Fig. 6(b), net quasiparticle recombination start in the RSS and the TPR-signal amplitude begins to decrease. As a sufficient number of quasiparticle recombine, the critical-current capacity increases and the sample returns to the ZRSS, time t_γ in Fig. 6(b), and a negative signal.

C. Thermalization from photoinduced normal and transition states

Given the small heat capacity of Nb below T_C, an increase in the photoabsorbed laser fluence can readily cause Nb to transition from the ZRSS, during the TPR-signal risetime (between t_0 and t_1 in Fig. 8), beyond the RSS into the transition or even the normal state. The TPR signal for these states is related to the temporal dependence of the sample's resistance $Z(t)$, see Secs. II and III. $Z(t)$ is dependent on the phonon density ϕ inside the film that is governed by the sample to substrate acoustic resistance, i.e., phonon trapping. Thus, the TPR signal, $E_{\text{osc}}(t) = Z(t)I_0$, has a slope which can be expressed as

$$\frac{dE_{\text{osc}}(t)}{dt} = I_0 \frac{dZ(t)}{d\phi} \frac{d\phi}{dt} . \tag{12}$$

The TPR-signal slope is a production of two derivatives: (1) the change in sample's impedance as a function of the phonon's quasistatic distribution (related to the temperature), and (2) temporal changes in the phonon distribution ($d\phi/dt$) dependent on the phonon escape rate into the substrate. The $d\phi/dt$ term remains relatively insensitive to temperature since it is primarily dependent on the substrate to film interface.[20,28–30,33]

In the normal state at higher temperatures (> 25 K), the resistance is linear with temperature, thus the $dZ(t)/d\phi$ term [see Eq. (12)] is approximated as a constant and $d\phi/dt$ determines the TPR-signal decay slope. At lower temperatures (< 25 K), the $dZ(t)/d\phi$ term becomes a much stronger function of temperature. Thus, the TPR-signal slope, as Nb thermalizes back to the

ZRSS, primarily corresponds to $dZ(t)/d\phi$. Using this model we analyze four cases in Figs. 8(a)–8(d).

In Fig. 8(a), the sample starts at t_0 in the ZRSS and experiences a photoinduced transition into the transition state by time t_1. Thermalization continues between times t_1 and t_2 when the sample cools through the transition state. Between times t_2 and t_3, Nb is thermalizing in the RSS [dashed curve in Fig. 8(a), inset]. From the R vs T inset in Fig. 8(a) it is evident that the largest derivative $dZ(t)/d\phi$ (i.e., largest slope) occurs between times t_1 and t_2 corresponding to the large impedance changes at T_C. This is followed by the sample entering the RSS, between times t_2 and t_3, where the dependence of impedance $dZ(t)/d\phi$ on the phonon density slows down and a slower TPR decay slope is observed.

This two-decay-slope TPR signal is expected from samples cooled to a temperature slightly below T_C. Conventionally, the resulting photoresponse is categorized as a combination[48,49] of a fast (nonbolometric) and slow (bolometric) thermalization process. However, the fast photoresponse slope is consistent with a bolometric[50] response since the observed different decay slopes are a manifestation of the nonlinear dependence of niobium's impedance on the phonon density $[dZ(t)/d\phi]$ near T_C.

Figure 8(b) occurs as more laser fluence photoinduces the sample to transition from the ZRSS (at time t_0) to the $T \leq 25$ K normal state (at time t_1). Niobium's nonlinear resistance versus temperature is approximated by two slopes [see inset in Fig. 8(b)]: one between T_C and ≈ 25 K and the other between ≈ 25 and 200 K. Between T_C and ≈ 25 K, the resistance does not change much with temperature since it is limited by scattering from impurities and from the film's surfaces. The resistance versus temperature slope between T_C and 25 K is about five times smaller than the slope between 25 and 200 K. Thermalization through a relatively temperature insensitive resistance region, between times t_1 and t_2, falsely appears as a delay in the niobium thermalization process. Once the niobium cools sufficiently to enter the transition temperature region, between times t_2 and t_3, the relaxation slope becomes steep as the impedance changes of niobium at T_C. Further thermalization transitions the sample at t_3 into the RSS [dashed curve in Fig. 8(b), inset].

Such a response is given in Fig. 9. A 20-nm Nb film on Al_2O_3 experiences a transition from the ZRSS into the normal state as it is heated by the laser's fluence from 6 to ≈ 17 K. The flat broad peak in Fig. 9 corresponds to cooling within the relatively temperature insensitive normal state towards T_C as is represented in Fig. 8(b) between times t_1 and t_2. This period does not correspond to a delay in the thermalization process but is a manifestation of the temperature-insensitive resistance of Nb between T_C and about 25 K.

Figure 8(c) occurs as the absorbed laser fluence increase the niobium temperature from the ZRSS (at t_0) into normal state and above ≈ 25 K by time t_1. Thermalization back to the RSS is not achieved within the 10-ns oscilloscope observation window. First the sample cools from the normal state above ≈ 25 K down to ≈ 25 K at about t_2. This cooling continues to below ≈ 25 K but never reaches T_C at about time t_3. Since the

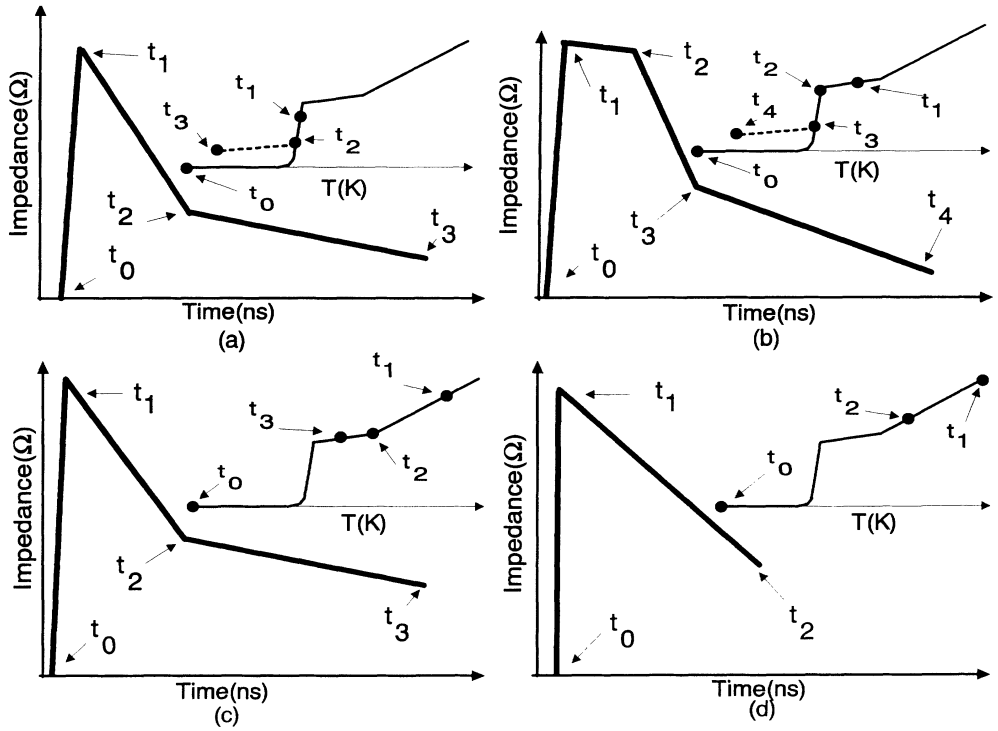

FIG. 8. Thermalization vs time ($t_0 < t_1 < t_2 < t_3 < t_4$) for niobium in the ZRSS undergoing various degrees of heating between t_0 and t_1.

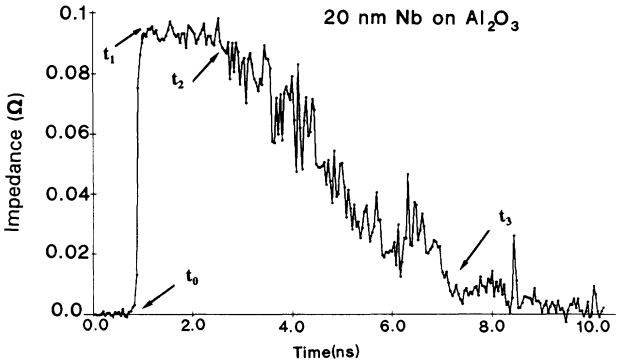

FIG. 9. The TPR signal from a 20-nm Nb film on an Al_2O_3 substrate biased with 80 mA and exposed to a 68 nJ laser fluence. Heating of this film from 6 to 13 K (between t_0 and t_1) produces the relatively broad flat peak [see Fig. 8(b)].

temperature-dependent [see inset 8(c)] resistance slope between time t_1 and t_2 is larger than between t_2 and t_3, the TPR signal exhibits two slopes starting with the larger slope, between t_1 and t_2, and continuing with a smaller slope between t_2 and t_3. This response is different from Fig. 8(a) as is evident from the TPR-signal amplitude. The TPR-signal amplitude, between t_2 and t_3, corresponds to the resistance above T_c and is significantly larger than the resistance in Fig. 8(a) between t_2 and t_3. An experimental TPR curve corresponding to this is shown in Fig. 5.

Figure 8(d) occurs for the highest laser fluences where the sample is heated from the ZRSS (at t_0) into the normal state at t_1. The heating is sufficiently larger to maintain the sample in the normal state and above 25 K within the 10-ns window it is observed. Since niobium does not thermalize sufficiently (between t_1 and t_2) to cool below 25 K a single TPR decay slope is observed. During the long time between laser pulses (500 μs), the sample returns to the ZRSS.

V. SUMMARY

The photoresponse of Nb was measured with the TPR technique[19,20] in the normal transition and superconducting states. The photoresponse was interpreted in terms of the thermalization of the photoexcited electrons by electron-electron and electron-phonon interactions and the phonon escape rate from the Nb film into the substrate. All the measurements reported on are extrinsic since they are strongly dependent on the phonon escape rate from the film into the substrate.

In the normal and transition states, the photoresponse is consistent with a bolometric model. The measured photoresponse amplitude agrees typically within a factor of 2 of the calculated values. In the normal state the TPR signal measured decay slope is four to five times larger than the calculated values from a simple acoustical model.[28–30] A slower decay is expected from nonideal niobium to substrate boundaries and has been observed previously for $YBa_2Cu_3O_7$ films.[20,33] The decay slope increases as T_C is approached. Given the narrow (50 mK) transition temperature of Nb, we were unable to maintain the sample exactly at T_C to measure the decay slope. Heating the sample with the laser fluence through T_C provided experimental photoresponse amplitude at T_C that agree very well with the calculated values.

Because of the small heat capacity, in the superconducting state niobium is very sensitive to laser fluence and readily transitions from the ZRSS into the RSS or the transition and normal states. At very low fluence the sample remains in the ZRSS and exhibits a positive signal for quasiparticle generation and a negative signal for quasiparticle recombination. The TPR-signal peak in the ZRSS is associated with rapid initial changes in the kinetic inductance. Phonons emitted during quasiparticle thermalization continue to increase the total number of broken pairs producing a positive TPR signal long after the laser pulse ceases. After a sufficient number of phonons escape into the substrate, recombination starts to dominate and a negative TPR signal is observed.

Given the small heat capacity of Nb at low temperature, photoabsorption can readily heat the sample into the transition or normal state during the TPR-signal risetime. The TPR signal exhibits several different decay slopes corresponding to the nonlinear dependence of the film's resistivity on temperature. The fastest slope is expected as the Nb sample cools from a normal state through the transition temperature to the RSS. Caution needs to be exercised if misrepresentation of this fast slope as quantum response is to be avoided.

Finally, it should be noted that the effective net quasiparticle generation and recombination lifetimes are much longer than expected from intrinsic predictions. The phonon trapping constriction at the film interface boundary dominates over and determines the measured quasiparticle lifetimes.

ACKNOWLEDGMENTS

The author is grateful to M. Johnson who helped with the measurements. I thank Joonhee Kang and John Talvacchio, who provided the Nb films, and to M. D. Fayer, in whose laboratory at Stanford University these measurements were made, and who provided the laser under NSF Grant No. DMR87-18959 and the Office of Naval Research, Physics Division, Grant No. N00014-89-J-1119. I wish to thank Bill Oldfield for technical assistance and S. R. Greenfield and J. J. Stankus for operating the laser. The advice of Ted Geballe, Malcolm Beasley, and Michal Reizer was greatly appreciated. I thank John Talvacchio and Martin Forrester for useful comments and suggestions. This work was supported in part by AFOSR Contract No. F49620-88-K-002 and by Westinghouse under task Z60601EHZB1.

[1]D. N. Langenberg (unpublished).
[2]S. B. Kaplan, C. C. Chi, D. N. Langenberg, J. J. Chang, S. Jafarey, and D. J. Scalapino, Phys. Rev. B **14**, 4854 (1976).
[3]A. Rothwarf and B. N. Taylor, Phys. Rev. Lett. **19**, 27 (1967).
[4]Jhy-Jiun Chang, in *Non-Equilibrium Superconductivity, Phonons, and Kapitza Boundaries,* edited by Kenneth E. Gray

(Plenum, New York, 1980), p. 263.
[5]A. M. Kadim and A. M. Goldman, *Modern Problems in Condensed Matter Sciences,* edited by V. M. Agranovich and A. A. Maradudin (Elsevier Science, Amsterdam, 1986), Vol. 12, p. 253.
[6]C. S. Owen and D. J. Scalapino, Phys. Rev. Lett. **28**, 1559 (1972).
[7]W. H. Parker and W. D. Williams, Phys. Rev. Lett. **29**, 924 (1972).
[8]J. Fuchs, P. W. Epperlein, M. Welte, and W. Eisenmenger, Phys. Rev. Lett. **38**, 919 (1977).
[9]W. H. Parker, Phys. Rev. B **12**, 3667 (1975).
[10]B. I. Miller and A. H. Dayem, Phys. Rev. Lett. **18**, 1000 (1967).
[11]M. Tinkham and John Clarke, Phys. Rev. Lett. **28**, 1366 (1972).
[12]G. J. Dolan and L. D. Jackel, Phys. Rev. Lett. **39**, 1628 (1977).
[13]W. J. Skocpol, M. R. Beasley, and M. Tinkham, J. Low Temp. Phys. **16**, 145 (1974).
[14]D. W. Jillie, J. E. Lukens, and Y. H. Kao, Phys. Rev. Lett. **38**, 915 (1977).
[15]L. R. Testardi, Phys. Rev. B **4**, 2189 (1971).
[16]J. Gittleman, B. Rosenblum, T. E. Seidel, and A. W. Wicklund, Phys. Rev. **137**, A527 (1965).
[17]R. Peters and H. Meissner, Phys. Rev. Lett. **30**, 965 (1973).
[18]Albert Schmid, Phys. Rev. **196**, 420 (1969).
[19]N. Bluzer, J. Appl. Phys. **71**, 1336 (1992).
[20]N. Bluzer, D. K. Fork, T. H. Geballe, M. R. Beasley, M. Y. Reizer, S. R. Greenfield, J. J. Stankus, and M. Fayer, IEEE Trans. Magn. **27**, 1519 (1991).
[21]N. Bluzer, Phys. Rev. B **44**, 10 222 (1991).
[22]M. Johnson, M. R. Beasley, T. H. Geballe, S. R. Greenfield, J. J. Stankus, and M. D. Fayer, Appl. Phys. Lett. **58**, 568 (1991).
[23]I. E. Leksina, in *Physical Acoustics and Optics,* edited by D. V. Skolbeltsyn (Consultants Bureau, New York, 1975), Vol. 72, p. 165.
[24]A. A. Abrikosov, L. P. Gorkov, and I. E. Dzyaloshinski, *Methods of Quantum Field Theory in Statistical Physics* (Prentice-Hall, Englewood, Cliffs, NJ, 1963).
[25]M. Y. Reizer, Phys. Rev. B **39**, 1602 (1989); **40**, 5411 (1989).
[26]The expressions for $\kappa=4\pi e^2\nu$ and $\beta=2\varepsilon_F\nu/3MNu_a^2$ are taken from Ref. 25. For a free-electron gas we approximate $\kappa\approx P_F$ and $\beta\approx 0.5$. The variables used to compute κ and β are ν the electronic two-spin density of states, M the ionic mass per unit cell, N the density of unit cells and u, the acoustic velocity.
[27]P. H. Dederichs, H. Schober, and D. J. Sellmyer, in *Numerical Data and Functional Relationship in Science and Technology,* edited by K. H. Hellwege and J. L. Olsen, Landott-Börnstein New Series, Vol. 13 (Springer-Verlag, Berlin, 1981), p. 96.
[28]W. A. Little, Can. J. Phys. **37**, 334 (1959).
[29]A. C. Anderson, in *Non-Equilibrium Superconductivity, Phonons, and Kapitza Boundaries* (Ref. 4).
[30]S. B. Kaplan, J. Low Temp. Phys. **37**, 343 (1979).
[31]A. C. Anderson and R. E. Peterson, Phys. Lett. **38A**, 519 (1972).
[32]J. D. N. Cheeke, H. Ettinger, and B. Herbal, Can. J. Phys. **54**, 1749 (1976).
[33]M. Nahum, S. Verghese, P. L. Richards, and K. Char, Appl. Phys. Lett. **59**, 2034 (1991).
[34]T. Klitsner and R. O. Pohl, Phys. Rev. B **36**, 6551 (1987).
[35]Y. S. Touloukian and E. H. Buyco, in *Thermophysical Properties of Matter: Specific Heat Metallic Elements and Alloys* (IFI/Plenum, New York, 1970), Vol. 4, p. 155.
[36]M. Tinkham, *Introduction to Superconductivity* (Krieger, Malabar, 1985), pp. 99 and 168.
[37]A. Schmid and G. Schon, J. Low Temp. Phys. **20**, 107 (1975).
[38]I. Schuller and K. E. Gray, Phys. Rev. Lett. **36**, 429 (1976).
[39]I. Schuller and K. E. Gray, Solid State Commun. **23**, 337 (1977).
[40]F. London, *Superfluids* (Wiley, New York, 1950), Vol. 1.
[41]N. Bluzer (unpublished); N. Bluzer and D. K. Fork, IEEE Trans. Magn. (to be published).
[42]B. L. Fielek, J. Phys. F **10**, 1665 (1980).
[43]Y. Nakagaw and A. D. B. Woods, in *Lattice Dynamics,* edited by R. F. Wallis (Pergamon, Oxford, 1965), p. 139.
[44]B. Friedl, C. Thomsen, and M. Cardona, Phys. Rev. Lett. **65**, 915 (1990).
[45]R. E. Cohen, W. E. Pickett, and H. Krakuer, Phys. Rev. Lett. **64**, 2575 (1990).
[46]R. E. Cohen, W. E. Pickett, and H. Krakuer, Phys. Rev. Lett. **62**, 831 (1989).
[47]B. W. Maxfield and W. L. McLean, Phys. Rev. B **139**, A1515 (1965).
[48]H. S. Kwok, J. P. Zheng, D. Y. Ying, and R. Rao, Appl. Phys. Lett. **54**, 2473 (1989).
[49]M. Johnson, Phys. Rev. Lett. **67**, 374 (1991); M. Johnson, N. Bluzer, M. Reizer, T. H. Geballe, S. R. Greenfield, J. J. Stankus, M. D. Fayer, and C. Herring, IEEE Trans. Magn. **27**, 1519 (1991).
[50]M. G. Forrester, M. Gottlieb, J. R. Gavaler, and A. I. Braginski, Appl. Phys. Lett. **53**, 3 (1988).